

# Green Chemistry

Accepted Manuscript



This is an *Accepted Manuscript*, which has been through the Royal Society of Chemistry peer review process and has been accepted for publication.

*Accepted Manuscripts* are published online shortly after acceptance, before technical editing, formatting and proof reading. Using this free service, authors can make their results available to the community, in citable form, before we publish the edited article. We will replace this *Accepted Manuscript* with the edited and formatted *Advance Article* as soon as it is available.

You can find more information about *Accepted Manuscripts* in the [Information for Authors](#).

Please note that technical editing may introduce minor changes to the text and/or graphics, which may alter content. The journal's standard [Terms & Conditions](#) and the [Ethical guidelines](#) still apply. In no event shall the Royal Society of Chemistry be held responsible for any errors or omissions in this *Accepted Manuscript* or any consequences arising from the use of any information it contains.

# **In-Situ Synthesis of Cotton-Derived Ni/C Catalysts with Controllable Structure and Enhanced Catalytic Performance**

Peng Zhang<sup>1</sup>, Zongbin Zhao<sup>1</sup>, Boris Dyatkin<sup>2</sup>, Chang Liu<sup>1</sup>, and Jieshan Qiu<sup>1\*</sup>

<sup>1)</sup> Carbon Research Laboratory, Liaoning Key Lab for Energy Materials and Chemical Engineering, State Key Lab of Fine Chemicals, School of Chemical Engineering, Dalian University of Technology, Dalian 116024, China

<sup>2)</sup> Department of Materials Science and Engineering, A. J. Drexel Nanotechnology Institute, Drexel University, Philadelphia, Pennsylvania 19104, USA

\*Corresponding Author. Tel: +86-411-84986080; E-mail: [jqiu@dlut.edu.cn](mailto:jqiu@dlut.edu.cn)

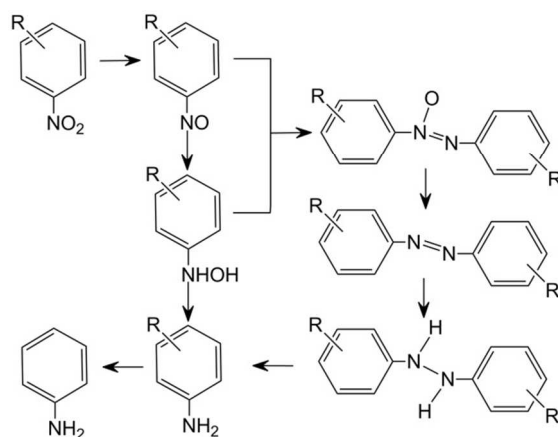
## Abstract

Owing to oxygen-driven hydrophilicity of the surface, cotton can absorb large amounts of aqueous solutions even at room temperature. We designed a facile two-step synthesis strategy that takes advantage of this property for in-situ fabrication of Ni/C catalysts with well-dispersed Ni particles on the carbonized cotton fiber. By tuning Ni loading and calcination temperatures, the size and distribution of Ni particles on the catalysts can be controlled. The catalytic performance of the as-made Ni/C catalysts has been tested for the selective hydrogenation of *o*-chloronitrobenzenes. It is found that the Ni/C catalyst obtained under the optimized conditions (51 wt% Ni loading, calcined at 400 °C) exhibits the best performance, with a yield of 100% in 5 h even at low H<sub>2</sub> pressure of 0.5 MPa. This new synthetic method may pave a way for producing low-cost Ni/C catalysts from cotton in large scale, which is attractive for industrial applications.

**Keywords:** cotton, Ni/C catalyst, hydrogenation reaction, green synthesis

## Introduction

Selective hydrogenation of chloronitrobenzenes (CNB) for subsequent chloroaniline (CAN) synthesis is widely used in commercial production of dyes, drugs, herbicides, and pesticides.<sup>1</sup> However, the pathways and mechanisms involved in this reaction are very complicated, and many toxic byproducts might be formed in this process (Scheme 1).<sup>2-5</sup> Although many noble metals such as Pt,<sup>6-9</sup> Pd,<sup>10, 11</sup> Au,<sup>12, 13</sup> Ag,<sup>14</sup> and Ru<sup>15</sup> catalysts have shown high conversion of CNB and selectivity to CAN in this reaction, excessive cost of those noble metals significantly limits the practicality of their implementation. As a result, many low-cost and sustainable catalysts have been studied as the promising catalysts for this reaction, such as Fe,<sup>16</sup> Fe<sub>2</sub>O<sub>3</sub>,<sup>17, 18</sup> and Co<sub>3</sub>O<sub>4</sub><sup>19, 20</sup>. Of various inexpensive catalysts, Ni catalysts,<sup>21-25</sup> which showcase high catalytic performance and affordability, have attracted substantial interest for the catalytic hydrogenation of CNB.



**Scheme 1.** The possible reaction process of the hydrogenation of CNB.

Generally, carbon materials have demonstrated good performance as the catalyst support substrates.<sup>26, 27</sup> In particular, they showcase robust intrinsic properties such as high specific

surface areas, unique electronic properties, and high chemical, thermal, and mechanical stabilities. However, synthesis of most carbon-based catalysts typically forgoes environmentally benign approaches in favor of complex and expensive procedures that include acid-oxidation, washing, impregnation, and reduction.<sup>22, 27</sup> In addition, the high cost of many novel carbon nanomaterials (such as graphene and carbon nanotube) makes their large-scale use less practical. Therefore, it is highly desirable to synthesize a cheap and effective Ni/C catalyst *via* facile and green strategies.

A common cash crop, cotton is mainly composed of cellulose fibers and is widely used for producing soft and breathable textiles and clothing.<sup>28</sup> The abundance, low price, and environmental sustainability of natural cotton make it highly practical for various applications.<sup>29, 30</sup> Recent research efforts have integrated cotton fabrics into synthesis pathways of several novel multifunctional materials, which have been successfully applied on many fields, such as energy storage and environmental protection.<sup>31-37</sup> To date, no cotton-derived functional materials have been implemented as catalyst supports. Herein, our novel approach uses the surface chemistry of cotton for designing a simple, green, and low-cost fabrication strategy of Ni/C catalysts. By controlling the Ni loading and the carbonization temperature, we can tune the dispersion, size, and distribution of Ni particles on carbon substrate matrices, further optimizing their catalytic performances for selective hydrogenation of *o*-CNB.

## Experimental

### Preparation of Catalysts

Medical absorbent cotton was adopted as the raw material and used without further purification,

which is named as CF. For a typical synthetic procedure, 0.5 g of cotton were ultrasonically dispersed in aqueous  $\text{Ni}(\text{NO}_3)_2$  solutions with different  $[\text{Ni}^{2+}]$  concentrations for 10 minutes to remove adhered air bubbles. Following a subsequent 24 h room temperature impregnation, the cotton- $\text{Ni}^{2+}$  material was removed and dried at 80 °C for another 24 h. The dried sample was loaded into a tube furnace and heated at 400 °C in  $\text{H}_2$  atmosphere for 3 h with a heating rate of 2 °C/min. The final black product was cooled back to room temperature. Respective to the 0.01 M, 0.05 M, 0.1 M, and 0.2 M initial  $[\text{Ni}^{2+}]$  concentrations, the corresponding products are hereafter referred to as 1-Ni/C, 2-Ni/C, 3-Ni/C, and 4-Ni/C (Table 1). For comparison, 0.5 g of cotton was directly treated by the standard calcination procedure, hereafter referred to as CCF.

### Characterization of Catalysts

The morphology and structure of as-obtained catalysts were characterized by scanning electron microscopy (SEM, Quanta 450) and X-ray diffraction (XRD, Rigaku D/Max-2400X,  $\text{Cu K}\alpha$  irradiation, operated at 40 kV and 100 mA). The Ni loading and elemental composition were established using inductively coupled plasma-optical emission spectrometers (ICP-OES, Optima 2000DV) and Elemental Analysis (EA, Elementar varioEL III). The size and dispersity of Ni particles in samples were measured using transmission electron microscopy (TEM) with a JEM-2000EX and averaged over 300 monodispersed Ni particles. Fourier Transform Infrared (FTIR) Spectrum was measured by a Thermo Nicolet 6700 Flex with an iTR attachment. Thermogravimetric analysis (TG) of CF was performed in a TA-Q50 in  $\text{N}_2$  atmosphere, in which the CF was heated from room temperature to 800 °C at a heating rate of 10 °C/min.

### Hydrogenation of *o*-Chloronitrobenzenes

The selective hydrogenation of *o*-CNB was carried out in a 100 mL Parr 4560 autoclave equipped with a mechanical stirrer. Typically, 0.05 g of milled catalyst was ultrasonically dispersed in 50 mL of ethanol combined with 0.5 g of *o*-CNB. Subsequently, the mixture was transferred into the Parr autoclave, completely sealed, and deaerated 3 times with pure H<sub>2</sub>. After an initial pressure of 0.5-1MPa H<sub>2</sub> was injected, the reactor was heated to 140 °C under constant stirring, and held at 140 °C for 3-5 h. Following the reaction, the autoclave was cooled back to room temperature and the mixture was separated by an external magnet. The solution was analyzed using gas chromatography (GC, Agilent 6890N chromatography, equipped with a SE-54 capillary column and a flame ionization detector), and the catalyst was ready for reuse after washing with ethanol and drying at 80 °C for 3h. The turnover frequency (TOF) was calculated on the basis of the total Ni amount and thus represents a conservative estimate.

**Table 1.** The average size of Ni particles and the Ni loading of Ni/C catalysts with corresponding initial solutions

Catalyst	[Ni <sup>2+</sup> ] (M)	Average size of Ni particles (nm)	Loading of Ni (wt %)
CCF	—	—	0
1-Ni/C	0.01	7.8	5.8
2-Ni/C	0.05	8.3	40.3
3-Ni/C	0.1	9.9	51.0
4-Ni/C	0.2	14.0	64.7

## Results and discussion

As a normal agricultural product, the natural cotton (Figure 1a) is comprised of multiple individual cotton fibers. Its representative morphology, which is shown in Figure 1b and c,

exhibits a typical spiral structure with diameters of 10-20  $\mu\text{m}$ . Every single cotton fiber is made of thousands of poly-D-glucose chains,<sup>28</sup> which are bound to each other *via* hydrogen bonding (Figure 1d).

FTIR analysis of the surface chemistry of CF in detail is shown in Figure 1e, and the spectrum shows a broad absorption peak in a range of 3335-3269  $\text{cm}^{-1}$  and featured peaks at 2892  $\text{cm}^{-1}$  and 1640  $\text{cm}^{-1}$ , which are assigned to the stretching vibrations of O-H in hydroxyl group, a C-H stretch, and C=C alkene groups, respectively. Additionally, a series of peaks at 1426-1107  $\text{cm}^{-1}$  and 1050-997  $\text{cm}^{-1}$  imply the presence of ester and carboxyl functionalities in CF.<sup>31</sup> This analysis demonstrates that a wide variety oxygen-containing groups are present on the surface of CF.

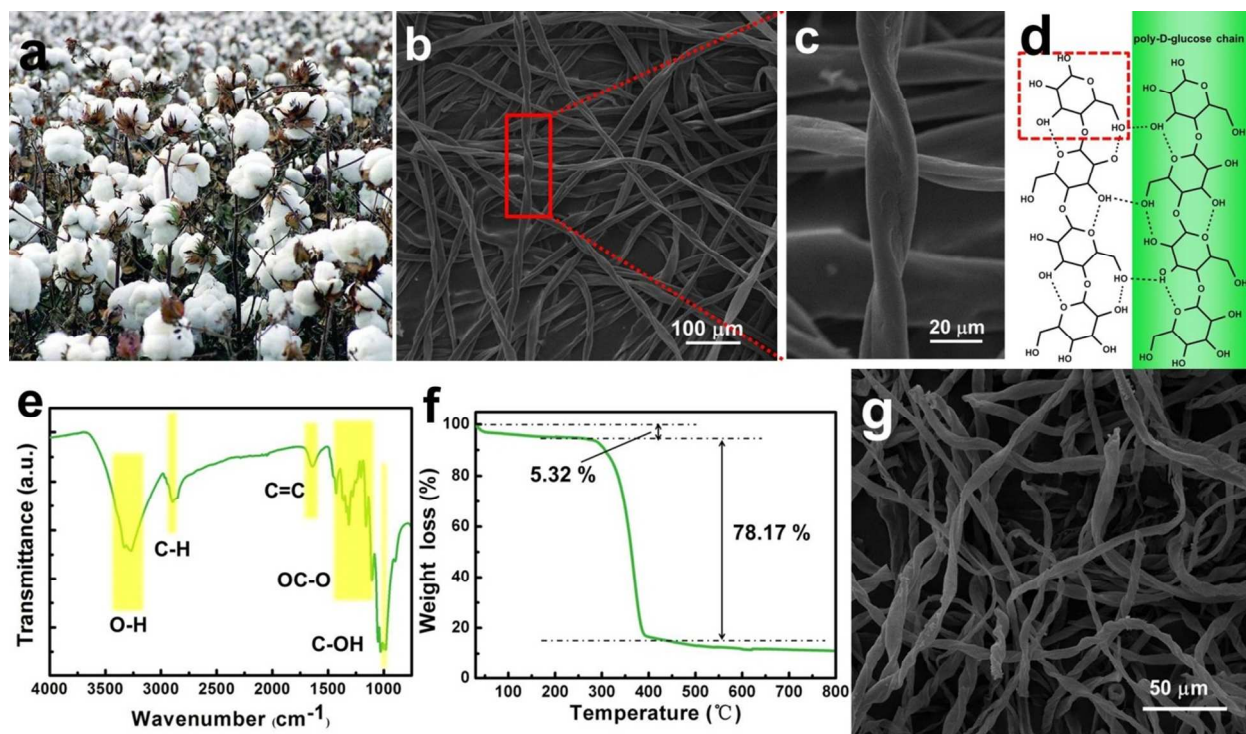


**Figure 1.** (a) A photograph of cotton field; (b) typical SEM image; (c) magnified SEM image; (d) molecular structure; (e) FTIR spectrum and (f) TG analysis in nitrogen of CF; (g) typical SEM image of CCF.



In order to investigate the thermal stability, the TG analysis of CF was measured, as shown in Figure 1f. The slight weight loss in mass below 250 °C is possibly attributed to the removal of water or gas from the surface, while the rapid loss in mass from 250 °C to 400 °C could be due to the pyrolysis of oxygen-containing groups in CF. EA of CF and CCF (Table S1) states that the C content elevates from 42.2% to 81.5% after calcination, while the O content decreases from 51.6% to 15.0%. Based on thermal and elemental analyses, we conclude that the CF can transform into a carbonized product and maintain thermal stability up to at least 400 °C; therefore, 400 °C was chosen as the lowest calcination temperature. The SEM image of CCF shows a retained spiral structure after calcining process, even though its diameter shrinks to 5-10  $\mu\text{m}$ , as shown in Figure 1g.

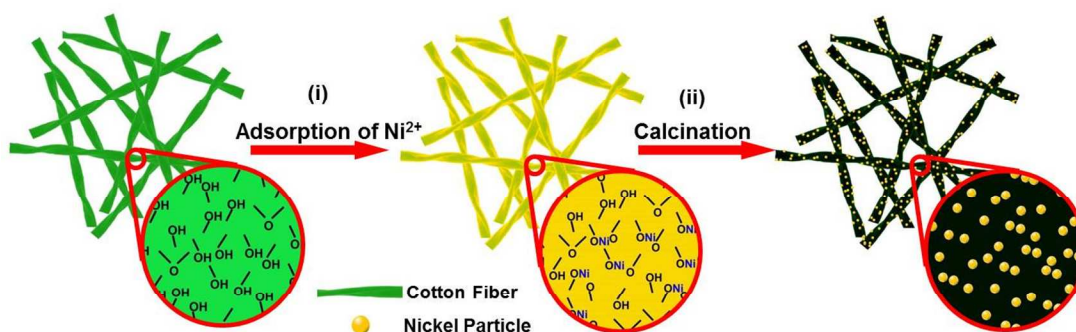


**Figure 2.** Schematic illustration of the synthesis of Ni/C catalysts.

The abundant oxygen-containing groups in cotton improve its hydrophilicity, increasing its absorption of large amounts of water or other polar solvents. As shown in Figure S1, 0.5 g of CF can adsorb about 12 mL of aqueous  $\text{Ni}(\text{NO}_3)_2$  solution after 24 h room temperature impregnation. Therefore, we designed a simple, green, and low-cost strategy to take advantage of cotton's

hydrophilicity and synthesize in situ Ni/C catalysts with controllable structures. This procedure involves two key steps, as shown in Figure 2: (i)  $\text{Ni}^{2+}$  ions in the initial solution are adsorbed onto the surface of CF at room temperature; (ii) The cotton-Ni<sup>2+</sup> material is calcinated at a high temperature in  $\text{H}_2$ , yielding the Ni/C catalyst with well-dispersed Ni particles. The cotton-derived products at different synthetic stages showcase different physical appearances, which could be observed from their digital photographs in Figure S1. This new method is scalable to industrial production levels and is sufficiently versatile to incorporate a wide range of metals for various metal/carbon or metallic oxide/carbon composites.

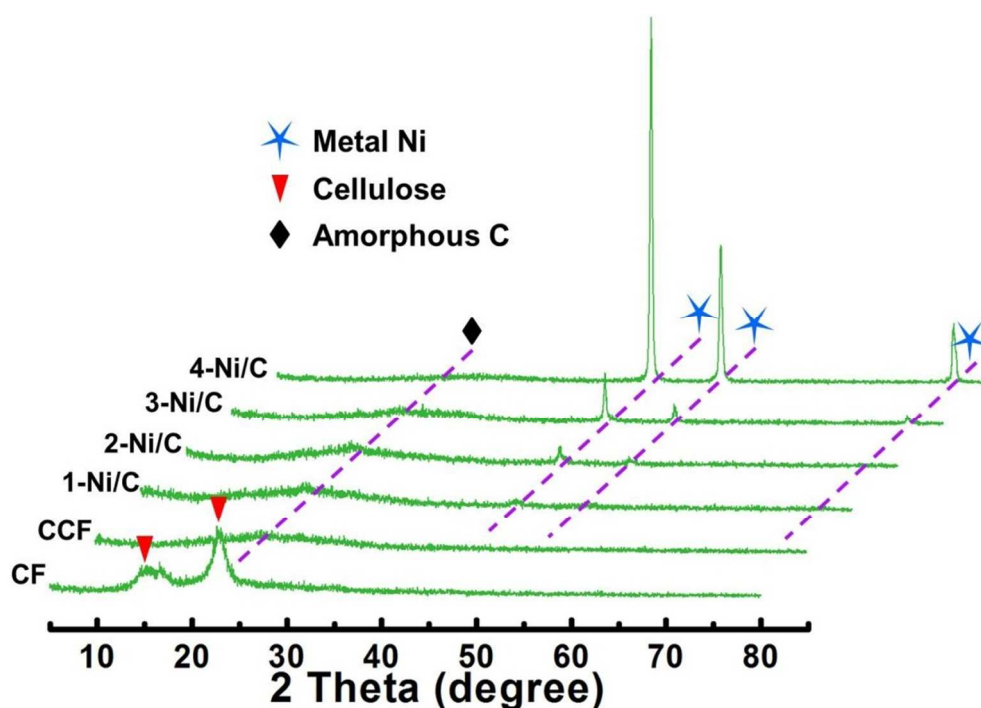


**Figure 3.** XRD patterns of CF, CCF and various Ni/C catalysts.

The XRD patterns of as-obtained samples (Figure 3) clearly show that two strong peaks at 15° and 23° in XRD pattern of CF disappear and a broad peak between 15° and 30° appears in CCF, indicating that the cellulose structure<sup>38</sup> in CF is destroyed and the amorphous carbon is formed

after high-temperature treatment. As for 1-Ni/C, 2-Ni/C, 3-Ni/C, and 4-Ni/C catalysts, besides the broad peak of amorphous carbon, three peaks at  $44.5^\circ$ ,  $51.8^\circ$  and  $76.4^\circ$  become prominent, corresponding to Ni (111), Ni (200), and Ni (220), respectively.<sup>22</sup> Therefore, we can conclude that the  $\text{Ni}^{2+}$  absorbed on CF has been thermally reduced to Ni and anchors itself on the carbon fibers *via* calcination.

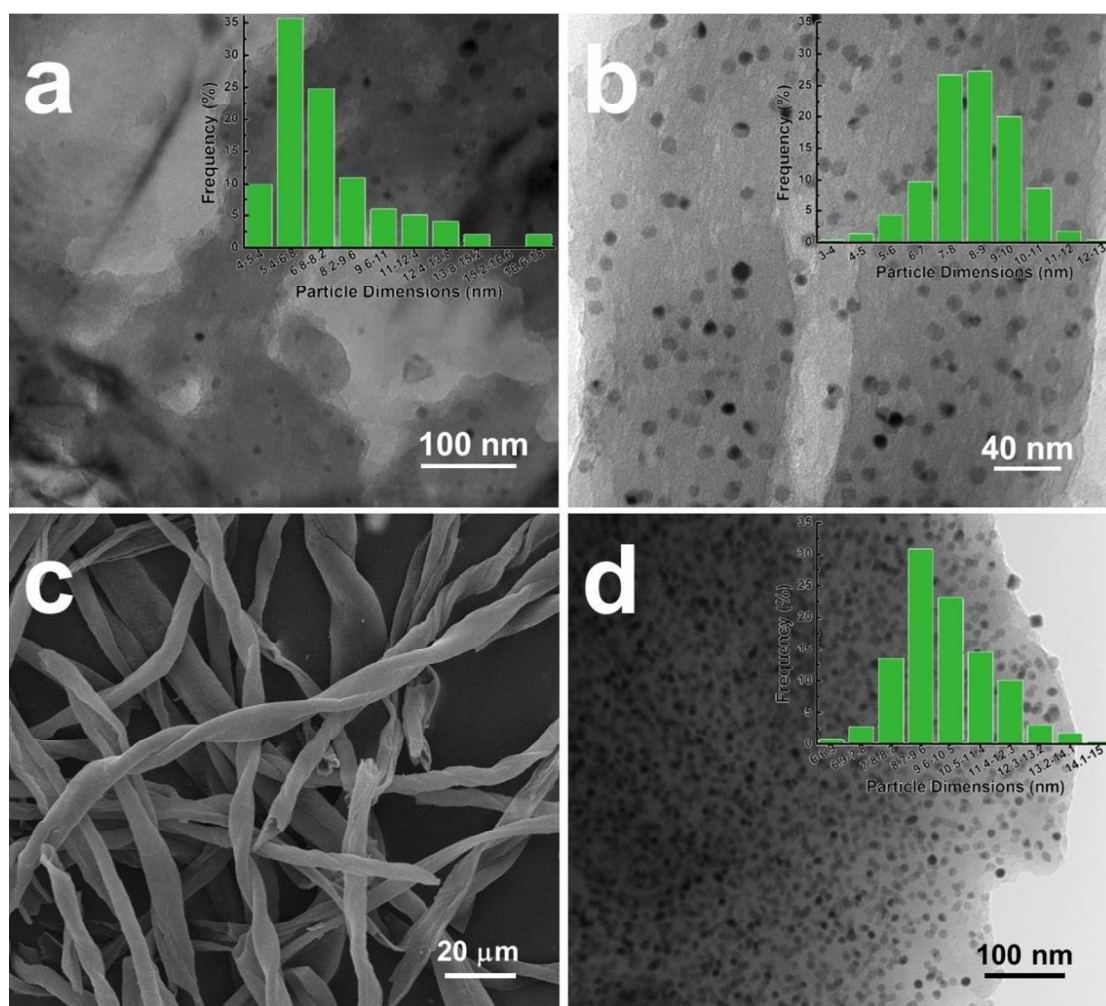


**Figure 4.** TEM images of (a) 1-Ni/C, (b) 2-Ni/C, and (d) 3-Ni/C, insets are the size distributions of Ni particles in corresponding catalysts; (c) typical SEM image of 3-Ni/C.

SEM images (Figure S2, S3, and 4c) show the morphologies of various Ni/C catalysts as

resembling spiral fibers with diameter in the range of 5-10  $\mu\text{m}$ . The generally similar sizes and uniform distribution of Ni particles can also be observed from the TEM images of three catalysts (Figure 4a, b and d). According to the ICP results and statistical data, the Ni loading and the average size of various Ni/C catalysts have been determined and summarized in Table 1. Compared with the 1-Ni/C and 2-Ni/C, it can be observed that a large number of small-sized Ni particles with 6-15 nm are densely and evenly supported on the carbon matrix of the 3-Ni/C, as shown in Figure 4d.

It should be noted that Ni overloading is not beneficial for the formation of the Ni/C catalysts with well-dispersed Ni particles. As the SEM image in Figure S4a shows, although the 4-Ni/C also retains a spiral fiber structure, the high Ni loading (about 64.7%) increases the apparent roughness of the surfaces (Figure S4b). The TEM image of the 4-Ni/C (Figure S4c) shows many agglomerated Ni particles with a wide distribution (4-42 nm, Figure S4d) on the carbon matrix. Hence, both poor dispersity and wide distribution of Ni particle sizes in the 4-Ni/C structure likely preclude catalytic performance, despite the ultrahigh Ni loading.

In addition to Ni loading, the calcination temperature also significantly affects the structure and catalytic performance of the Ni/C catalysts. A series of 3-Ni/C catalysts thermally-treated at 200  $^{\circ}\text{C}$ -600  $^{\circ}\text{C}$  were prepared, which are hereafter referred as 3-Ni/C-t ("t" refers to the calcination temperature). Unlike previous samples that showcased predominantly black coloring, the 3-Ni/C-200 has a brown appearance (insert of Figure 5a), and XRD analysis (Figure 5a) confirms a structure that is almost identical to that of the CF. However, it is observed that the featured peaks of metal Ni exist in XRD patterns of other catalysts (Figure S5), indicating that

the  $\text{Ni}^{2+}$  adsorbed onto the cotton surface can be transformed into metal Ni at 300 °C or above. On the other hand, higher calcination temperatures promote the growth and agglomeration of Ni particles, damaging their dispersity. TEM images of the 3-Ni/C-300, 3-Ni/C-500 and 3-Ni/C-600 (Figure 5b, c, and d) show that the Ni particle sizes on catalysts are gradually increasing and the size distributions are widening (inserts of Figure 6b, c and d) with the increase of calcination temperature. As a result, the bigger size and wider distribution of Ni particles on the 3-Ni/C-500 and 3-Ni/C-600 predict the decreased catalytic performance compared with the 3-Ni/C-400.

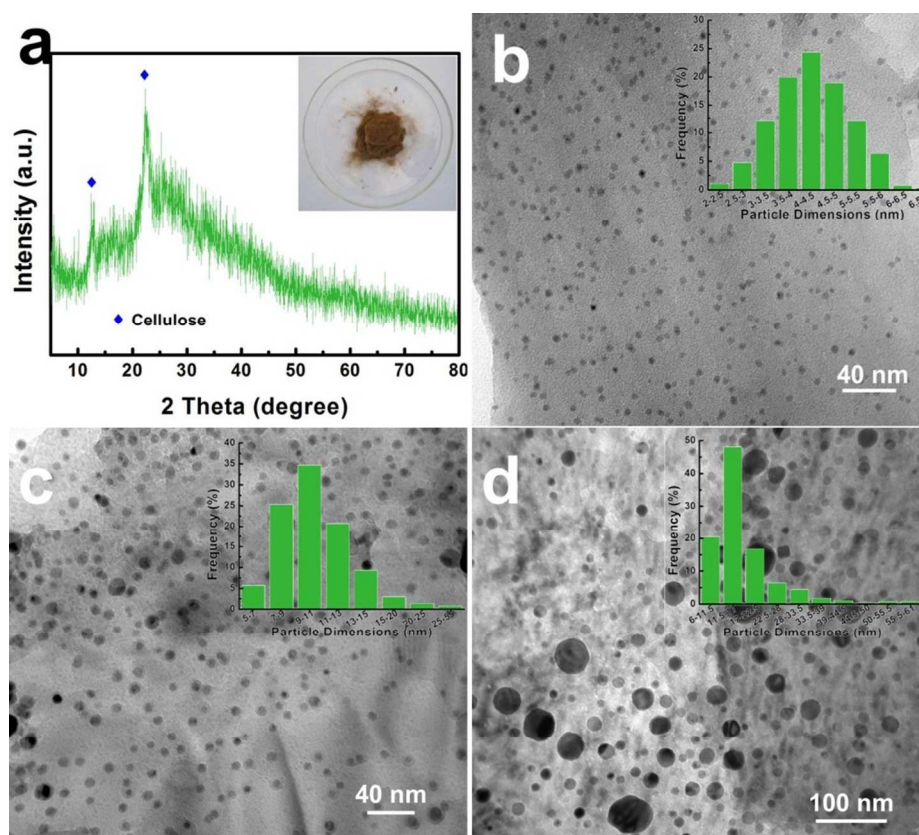


**Figure 5.** (a) XRD pattern of 3-Ni/C-200, insert is its photograph; TEM images of (b) 3-Ni/C-300, (c) 3-Ni/C-500 and (d) 3-Ni/C-600, insets are the size distributions of Ni particles in corresponding catalysts.



The catalytic performance of Ni/C catalysts with different Ni loadings for selective hydrogenation of *o*-CNB was investigated in detail, as shown in Figure 6a and Table S2. Compared with others, the 3-Ni/C obviously exhibits the highest catalytic activity under the same reaction conditions, and a full conversion of *o*-CNB can be finished in 5 h even at low pressures of H<sub>2</sub> (0.5 MPa). To date, Ni-based catalysts have not exhibited such high catalytic activity for hydrogenation of CNB at such low H<sub>2</sub> pressures.<sup>21-24</sup> As discussed above, the poor catalytic performances of the 1-Ni/C and 2-Ni/C are mainly due to their low Ni loading and insufficient catalytic active sites, while the decreased *o*-CNB conversion over the 4-Ni/C is mainly attributed to large diameters and poor dispersion of Ni particles. Furthermore, all Ni/C catalysts obtained in the present work exhibit high selectivities to *o*-CAN, regardless of different catalytic performance.

As for the 3-Ni/C catalysts calcined at different temperatures, their catalytic performances were also tested under the aforementioned reaction conditions, as shown in Figure 6b and Table S3. As expected, the 3-Ni/C-200 reached negligible *o*-CNB conversion, owing to the inability of reduction of Ni<sup>2+</sup> on the CF surface into metallic Ni at 200 °C. Compared with the 3-Ni/C-300 and 3-Ni/C-400, the decreasing catalytic activities of the 3-Ni/C-500 and 3-Ni/C-600 mainly result from the growth and agglomeration of Ni particles at the highest calcination temperatures. As for the 3-Ni/C-300, it is not the appropriate catalyst in the present work, although it shows the equally catalytic performance with the 3-Ni/C-400. As shown by the TG results (Figure 1f), the CF cannot be transformed into the stable carbon matrix at temperatures below 400 °C. At 300 °C,

some impurities are released into the reaction solution and pollute the product, resulting in a dark-brown solution after the reaction (Figure S5). Therefore, 400 °C is the optimum calcination temperature for the formation of Ni/C catalysts with the perfect structure and the best catalytic performance.

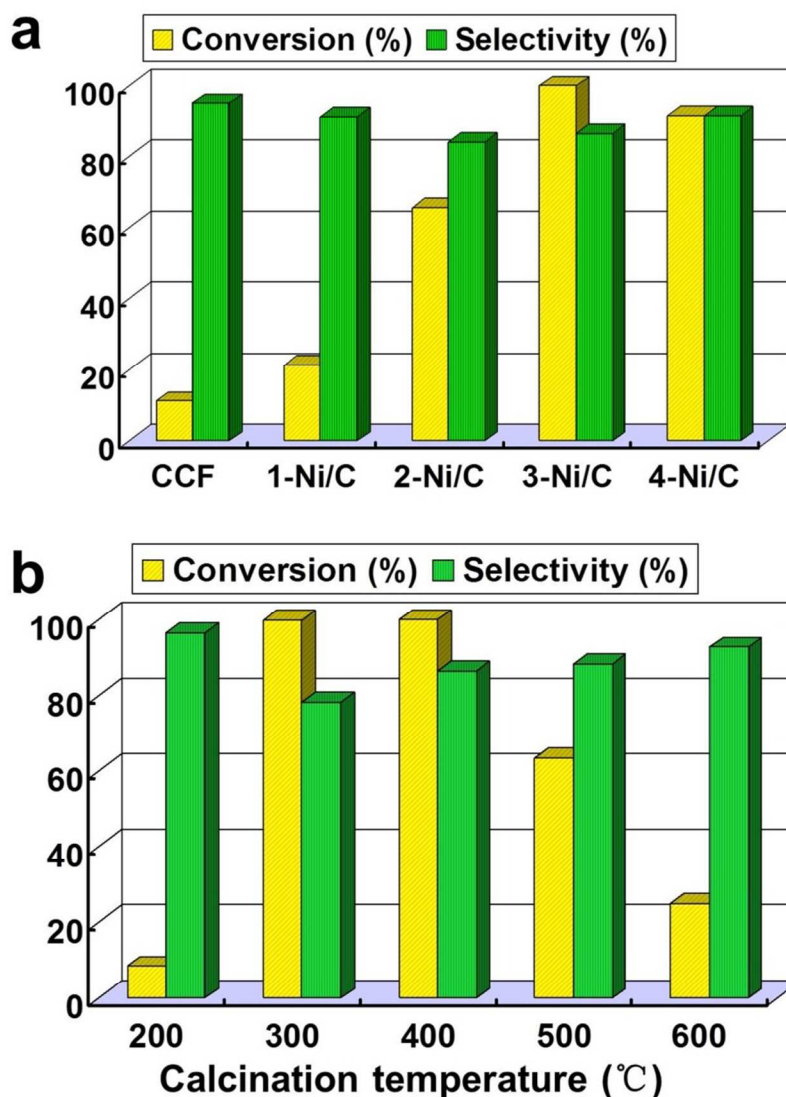


**Figure 6.** The catalytic performance of (a) various Ni/C catalysts and (b) 3-Ni/C catalysts calcined at different temperature for the selective hydrogenation of *o*-CNB. Reaction conditions:

0.50 g *o*-CNB, 0.05 g catalyst, 50 mL ethanol, 140 °C, 0.5 MPa H<sub>2</sub>, 5 h.

Because of the unique magnetic property of metal Ni in Ni/C catalysts, they can be conveniently recovered by an external magnet after the hydrogenation reaction (inset of Figure S7). Repeated reaction cycling (Figure S7 and Table S4) demonstrates a good stability of the 3-Ni/C, over which above 70% conversion of *o*-CNB has been maintained after six reaction cycles, meanwhile the selectivity to *o*-CAN does not fall below 90%. It is interesting to note that the *o*-CNB conversion decreases after 3 cycles, probably due to the aggregation of a little amount of unstable Ni particles, which is inevitably formed during the synthesis of Ni/C catalysts. In order to figure out the reason behind the deactivation, the 3-Ni/C is recovered after 6 cycles and characterized by ICP and TEM. The results have shown that the reused catalyst has an identical Ni loading (51.9 %) with the flash catalyst and increasing size of Ni particles (Figure S8), indicating the decreasing catalytic activity of the 3-Ni/C is mainly due to the aggregation of Ni particles, not due to the leaching loss of Ni content.

## Conclusions

A simple, green and low-cost synthetic strategy involving the absorption and calcination step has been developed to in-situ fabricate Ni/C catalysts with well-dispersed Ni particles with cotton as the carbon precursor. The size and distribution of Ni particles on the carbon matrix can be tuned by controlling the Ni loading and the carbonization temperature, which have an impact on the catalytic performance of the Ni/C catalysts for the selective hydrogenation of *o*-CNB. It has been found that the 3-Ni/C catalyst with high Ni loading and well-dispersed Ni particles of 6-14 nm in diameter has high catalytic performance for completely converting *o*-CAN in 5 h even at low 0.5 MPa H<sub>2</sub> pressure. This synthetic method is easy to scale up to produce the eco-friendly Ni/C



catalysts that hold significant promise in large scale applications.

## Electronic Supplementary Information

Elemental compositions of CF and CCF. The digital photographs during the synthesis process of Ni/C catalysts. SEM images of 1-Ni/C, 2-Ni/C, and 4-Ni/C. TEM image of 4-Ni/C. Size distributions of Ni particles of 4-Ni/C. XRD patterns of 3-Ni/C catalysts calcined at different temperature. Catalytic performance of various Ni/C catalysts and 3-Ni/C with different calcination temperatures for the selective hydrogenation of *o*-CNB. The digital photographs of reaction solutions before and after the hydrogenation of *o*-CNB. Cycling performance of 3-Ni/C for selective hydrogenation of *o*-CNB. TEM image of the 3-Ni/C after 6 cycles.

## Acknowledgements

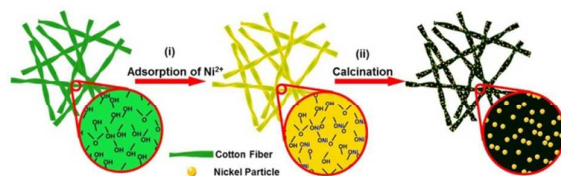
This work was partly supported by the NSFC (Nos. 21336001, 21361162004), and the Education Ministry of China (No.20120041110020). B. Dyatkin thanks the support from the IMI Program of the National Science Foundation under Award (No. DMR 08-43934).

## Notes and references

1. H. Blaser, H. Steiner and M. Studer, *ChemCatChem*, 2009, **1**, 210-221.
2. A. Corma, P. Concepcion and P. Serna, *Angew. Chem. Int. Ed.*, 2007, **46**, 7266-7269.
3. E. Gelder, D. Jackson and M. Lok, *Chem. Commun.*, 2005, 522-524.
4. X. Meng, H. Cheng, S.-i. Fujita, Y. Yu, F. Zhao and M. Arai, *Green Chem.*, 2011, **13**, 570-572.
5. J. Ning, J. Xu, J. Liu, H. Miao, H. Ma, C. Chen, X. Li, L. Zhou and W. Yu, *Catal. Commun.*, 2007, **8**, 1763-1766.
6. C. Lian, H. Liu, C. Xiao, W. Yang, K. Zhang, Y. Liu and Y. Wang, *Chem. Commun.*, 2012, **48**, 3124-3126.
7. F. Wang, J. Liu and X. Xu, *Chem. Commun.*, 2008, 2040-2042.
8. Y. Xie, C. Yu, N. Xiao and J. Qiu, *Catal. Commun.*, 2012, **28**, 69-72.
9. X. Xu, X. Li, H. Gu, Z. Huang and X. Yan, *Appl. Catal. A*, 2012, **429-430**, 17-23.
10. V. Kratky, M. Kralik, M. Mecarova, M. Stolcova, L. Zalibera and M. Hronec, *Appl. Catal. A*, 2002, **235**, 225-231.
11. Y.-M. Lu, H.-Z. Zhu, W.-G. Li, B. Hu and S.-H. Yu, *J. Mater. Chem. A*, 2013, **1**, 3783-3788.

12. Y. Chen, J. Qiu, X. Wang and J. Xiu, *J. Catal.*, 2006, **242**, 227-230.
13. D. He, H. Shi, Y. Wu and B.-Q. Xu, *Green Chem.*, 2007, **9**, 849-851.
14. Y. Chen, C. Wang, H. Liu, J. Qiu and X. Bao, *Chem. Commun.*, 2005, 5298-5300.
15. B. Zuo, Y. Wang, Q. Wang, J. Zhang, N. Wu, L. Peng, L. Gui, X. Wang, R. Wang and D. Yu, *J. Catal.*, 2004, **222**, 493-498.
16. R. Jagadeesh, G. Wienhofer, F. Westerhaus, A. Surkus, M. Pohl, H. Junge, K. Junge and M. Beller, *Chem. Commun.*, 2011, **47**, 10972-10974.
17. R. Jagadeesh, K. Natte, H. Junge and M. Beller, *ACS Catal.*, 2015, **5**, 1526-1529.
18. R. Jagadeesh, A. Surkus, H. Junge, M. Pohl, J. Radnik, J. Rabeah, H. Huan, V. Schünemann, A. Brückner and M. Beller, *Science*, 2013, **342**, 1073-1076.
19. R. Jagadeesh, D. Banerjee, P. Arockiam, H. Junge, K. Junge, M. Pohl, J. Radnik, A. Brückner and M. Beller, *Green Chem.*, 2015, **17**, 898-902.
20. F. Westerhaus, R. Jagadeesh, G. Wienhofer, M. Pohl, J. Radnik, A. Surkus, J. Rabeah, K. Junge, H. Junge, M. Nielsen, A. Bruckner and M. Beller, *Nat. Chem.*, 2013, **5**, 537-543.
21. X. Meng, H. Cheng, S.-I. Fujita, Y. Hao, Y. Shang, Y. Yu, S. Cai, F. Zhao and A. Masohiko, *J. Catal.*, 2010, **269**, 131-139.
22. C. Wang, J. Qiu, C. Liang, L. Xing and X. Yang, *Catal. Commun.*, 2008, **9**, 1749-1753.
23. J. Wang, G. Fan and F. Li, *Catal. Sci. Technol.*, 2013, **3**, 982-991.
24. J. Xiong, J. Chen and J. Zhang, *Catal. Commun.*, 2007, **8**, 345-350.
25. P. Zhang, C. Yu, X. Fan, X. Wang, Z. Ling, S. Wang and J. Qiu, *Phys. Chem. Chem. Phys.*, 2015, **17**, 145-150.
26. P. Serp, M. Corrias and P. Kalck, *Appl. Catal. A*, 2003, **253**, 337-358.
27. M. Oubenali, G. Vanucci, B. Machado, M. Kacimi, M. Ziyad, J. Faria, A. Raspolli-Galetti and P. Serp, *ChemSusChem*, 2011, **4**, 950-956.
28. M. Lewin, *Handbook of Fiber Chemistry*, CRC Press, Boca Raton, 2007.
29. A. G. Avila, J. P. Hinstroza and J. H. Xin, *Nat. Nanotechnol.*, 2008, **3**, 458-459.
30. R. F. Service, *Science*, 2003, **301**, 909-911.
31. L. Bao and X. Li, *Adv. Mater.*, 2012, **24**, 3246-3252.
32. H. Bi, Z. Yin, X. Cao, X. Xie, C. Tan, X. Huang, B. Chen, F. Chen, Q. Yang, X. Bu, X. Lu, L. Sun and H. Zhang, *Adv. Mater.*, 2013, **25**, 5916-5921.
33. L. Hu, M. Pasta, F. L. Mantia, L. Cui, S. Jeong, H. D. Deshazer, J. W. Choi, S. M. Han and Y. Cui, *Nano Lett.*, 2010, **10**, 708-714.
34. K. Jost, C. R. Perez, J. K. McDonough, V. Presser, M. Heon, G. Dion and Y. Gogotsi, *Energy Environ. Sci.*, 2011, **4**, 5060-5067.
35. Y. Liu, X. Wang, K. Qi and J. H. Xin, *J. Mater. Chem.*, 2008, **18**, 3454-3460.
36. J. Xue, Y. Zhao, H. Cheng, C. Hu, Y. Hu, Y. Meng, H. Shao, Z. Zhang and L. Qu, *Phys. Chem. Chem. Phys.*, 2013, **15**, 8042-8045.
37. G. Yu, L. Hu, M. Vosgueritchian, H. Wang, X. Xie, J. R. McDonough, X. Cui, Y. Cui and Z. Bao, *Nano Lett.*, 2011, **11**, 2905-2911.
38. E. Csiszar and E. Fekete, *Langmuir*, 2011, **27**, 8444-8450.

## Table of Contents



Due to the good hydrophilicity of natural cotton, a simple, green, and low-cost strategy has been designed to in-situ fabricate the Ni/C catalysts with controllable structure and catalytic performance.